# Design and performance analysis of a long-stroke electromagnetic double-reel hammer

**Jawdat S. Alkasassbeh[1], Vlademer E. Pavlov[2], Khalaf Y. Al-Zyoud[1], Tareq A. Al-Awneh[1], Osamah Alkasassbeh[3], Ayman Y. Al-Rawashdeh[1]**

[1]Department of Electrical Engineering, Faculty of Engineering Technology, Al-Balqa Applied University, Amman, Jordan
[2]Department of Mechatronics Engineering, Irkutsk National Research Technical University, Irkutsk, Russia
[3]Department of Physics, Faculty of Science, Mutah University, Al-Karak, Jordan

| Article Info | ABSTRACT |
|---|---|
| | This paper comprehensively investigates the performance characteristics of a long-stroke electromagnetic double-reel hammer compared to a conventional hammer. Quantitative analysis indicates that the long-stroke hammer shows a significant increase in striker speed and impact energy. The impact energy has increased by 255%, and energy losses in copper windings have decreased by 124% per operating cycle. Additionally, the long-stroke hammer demonstrates a 105% reduction in energy consumption and a 52% improvement in overall efficiency per cycle compared to the conventional hammer. This study examines the operational characteristics of the long-stroke hammer throughout its cycle using field theory methods, MATLAB simulations, and experimental tests. Results indicate higher impact energy and speed, lower energy losses in copper windings, and higher efficiency per cycle for the long-stroke hammer. Furthermore, a mathematical model of the long-stroke hammer is developed, incorporating static parameters and oscillograms of striker movement and current flow. A comprehensive comparison of the performance indicators of both hammers reveals significant improvements in lifting height, cycle duration, impact frequency, and striker speed for the long-stroke hammer. Overall, these findings suggest that the long-stroke operating mode can significantly enhance the efficiency and performance of conventional hammers while simultaneously reducing impact frequency and machine heating.<br><br>*This is an open access article under the CC BY-SA license.* |

*Corresponding Author:*

Jawdat S. Alkasassbeh
Department of Electrical Engineering, Faculty of Engineering Technology, Al-Balqa Applied University
Amman, Jordan
Email: jawdat1983@bau.edu.jo

## 1. INTRODUCTION

The long-stroke electromagnetic hammer stands at the forefront of industrial innovation, embodying a fusion of precision engineering and advanced electromagnetic technology. This specialized tool is designed to deliver controlled and powerful impact forces over extended stroke lengths, catering to a wide array of applications in material processing, construction, and manufacturing industries. By harnessing electromagnetic principles, the long-stroke hammer offers a unique blend of force, accuracy, and adjustability, setting it apart from traditional hammer designs [1], [2]. In the realm of industrial tools, the long-stroke electromagnetic hammer represents a paradigm shift, enabling users to achieve high-precision impact operations with unparalleled efficiency. Through the utilization of electromagnetic fields to propel the

hammer mechanism through extended strokes, this tool exemplifies a harmonious balance between power and control, making it a versatile asset in various industrial settings [3].

The exploration of the long-stroke electromagnetic hammer delves into its operational intricacies, design considerations, and performance capabilities. By unraveling the underlying principles governing its functionality, this introduction aims to shed light on the technological advancements driving the evolution of electromagnetic hammer technology. Through a synthesis of theoretical insights and practical applications, this study seeks to provide a comprehensive understanding of the operational dynamics and performance factors influencing the long-stroke electromagnetic hammer [4].

Many published papers are dedicated to optimizing the utilization of linear electromagnetic propulsion across various technological domains [5]-[9]. Among these technologies, electromagnetic effect machines, a specialized class of electrical machinery, find extensive application in industry, particularly in the implementation of pulse technologies. Notably, one intriguing facet of the historical trajectory of electromagnetic impact machines is their diverse range of energy outputs, with individual units capable of delivering impact energies up to 100 kJ and power outputs reaching 40 kW. These electromagnetic impact machines, colloquially known as electromagnetic hammers, serve multifarious purposes including rock demolition, pile driving, permafrost development, offshore oilfield construction, and as sources of vibration in downhole operations [10], [11]. An inherent objective in the development of such hammers lies in augmenting energy efficiency throughout their operational lifecycle. The challenges of energy optimization in electromagnetic impact machines are notably intricate [12], [13], as the efficiency of energy conversion intricately hinges upon the delineation of their operational cycles.

Significant contributions to the structuring of the operational cycles of electromagnetic machinery are evident in the works of [14], [15]. Adherence to these guidelines promises to maximize the operational speed of the machine or ensure its optimal efficiency. Noteworthy among electric hammers are those developed by the Institute of Mining of the Siberian Branch of the Russian Academy of Sciences [16], [17]. They are distinguished by their simplistic design, heightened operational reliability, minimal environmental impact (devoid of exhaust emissions), and reliance on cost-effective energy sources. A notable variant, the long-stroke electromagnetic hammer as shown in Figure 1, distinguishes itself from conventional two-reel hammers by integrating two guide pipes and additional striker position sensors to enhance impact energy through increased striker velocity. Further details regarding the components visible in Figure 1 are provided in Table 1.
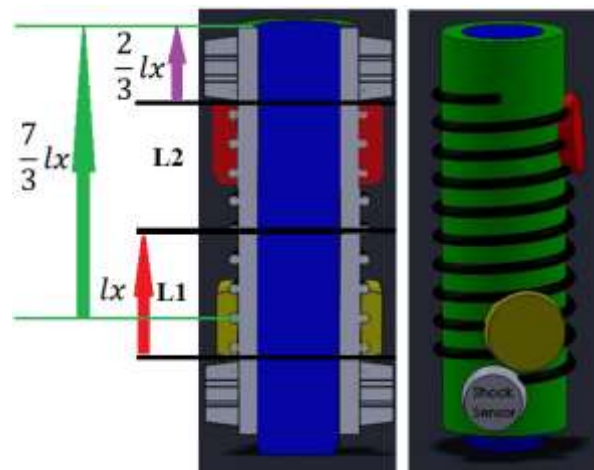


Figure 1. The long-stroke electromagnetic hammer

Table 1. The parts of a long-stroke electromagnetic hammer in Figure 1

| Color code | Part name |
| --- | --- |
| Sliver | Shock sensor |
| Green | Guide pipe |
| Blue | Striker |
| Yellow | Striker lower and upper position sensor |
| Black | Electromagnetic coil |
| Red | Striker upper position sensor |

Figure 2 shows the block diagram of the control of a long-stroke electromagnetic hammer, which contains control unit B, controlled rectifiers V1 and V2, and striker position sensors SN1 and SN4. Control unit B orchestrates the interplay between the signal driving devices (Um1, Um2) and the striker position sensors (SN1, SN2, SN3, and SN4). Initially, the firing pin resides in its lowest position. Upon the application of a task voltage to initiate the rectifier mode operation of the controlled rectifier V1, the striker is drawn into the coil of electromagnet L1. As the lower edge of the striker disengages from the lower-position sensor SN2, a signal prompts the transition of V1 into inverter mode, simultaneously activating the controlled rectifier V2 in rectifier mode. Consequently, the current in the coil of electromagnet L1 diminishes, while that in the coil of electromagnet L2 escalates, facilitating the striker's movement into the latter coil. As the upper edge of the striker nears the upper position sensor SN3, V2 is switched to inverter mode, nullifying the current in the coil of electromagnet L2. The striker's upward trajectory continues propelled by its accumulated kinetic energy until it approaches the uppermost position sensor SN4, prompting V2 to transition to rectifier mode, thus drawing the striker into the coil of electromagnet L2. The downward movement of the striker triggers the upper position sensor SN3, activating controlled rectifier V1 and transitioning V2 into inverter mode, thereby nullifying the current in the coil of electromagnet L2 and initiating the striker's movement towards electromagnet L1. As the bottom edge of the striker approaches the lower-position sensor SN2, V1 transitions to inverter mode, halting the current in the coil of electromagnet L1. Subsequently, the striker continues its downward trajectory, driven by its kinetic energy. Upon nearing the impact sensor SN1, a signal prompts V1 to transition to rectifier mode, facilitating the striker's retraction into the coil of electromagnet L1 upon impact. This operational cycle of the long-stroke electromagnetic hammer recurs systematically.
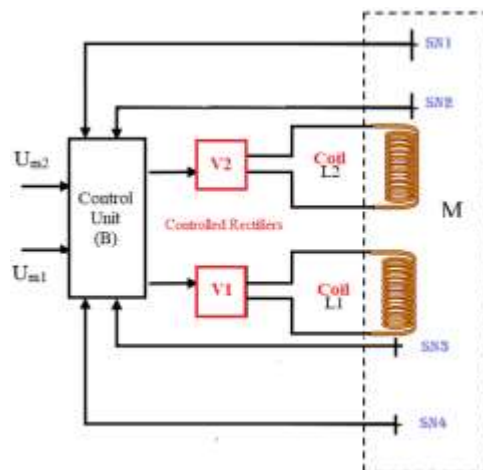


Figure 2. The block diagram of the control of a long-stroke electromagnetic hammer

The primary operating modes of a long-stroke electromagnetic double-reel hammer encompass:
− Striker mode: starting the moving part of the machine.
− Moving mode: striker to the initial upper position when alternately switching two windings.
− Deceleration mode: stopping the striker in the initial upper position.
− Operating mode: alternating switching of two windings.

The movement of a striker begins when the machine's traction force equals the resistance to movement force. The duration, energy intensity, frequency of impacts, and machine efficiency depend on the machine's traction force. In idle mode, the firing pin accumulates potential energy, which is converted into kinetic energy throughout the employed stroke. The stored potential energy and impact energy are directly proportional, and the frequency of impacts is inversely proportional to the striker's stroke. Adjusting the striker's stroke can adjust the energy and frequency of impacts. The efficiency of energy conversion at each point of the striker's trajectory is determined by the ratio of these quantities. Deceleration and stopping during idle can occur due to braking forces of resistance and braking devices. The striker builds up potential energy as they travel slowly, which they can partially utilize during the working stroke. The striker accumulates potential energy as it moves at a slow pace, which can be partially harnessed during the active stroke. The extent of the striker's stroke, the duration of deceleration, and the frequency and energy of machine impacts are contingent upon the initiation and intensity of the deceleration mode. During the power

stroke mode, the engine utilizes the potential energy accumulated during idle time, which then transforms into kinetic energy upon movement. Additionally, kinetic energy can be augmented by the traction forces generated when the two windings are activated and deactivated throughout the power stroke. The fundamental feature of electromagnetic impact machines is their operation in dynamic modes, while the machine and a power static converter form a purely nonlinear electromechanical system. Therefore, the analysis of dynamic modes, taking into account the main nonlinearities, presents significant difficulties. MATLAB Simulink is presently employed to analyze systems' objects of nearly any complexity level [18]. One significant benefit of this approach is the capacity to see and track progress over some time. The objective of this study is to quantitatively evaluate the operational and energy characteristics of a long-stroke electromagnetic double-reel hammer. The main contributions of this paper can be summarized as follows:

− Quantitative analysis: the paper provides quantitative estimates, revealing significant improvements in the performance metrics of the long-stroke hammer. These include a 255% increase in impact energy and a 124% reduction in energy losses in copper windings per operating cycle. Additionally, the long-stroke hammer exhibits a remarkable 105% reduction in energy consumption and a 52% improvement in overall efficiency per cycle compared to the conventional hammer.

− Investigation of operating characteristics: the study delves into the impact energy and efficiency of a long-stroke electromagnetic double-reel hammer throughout its operating cycle. By employing field theory methods, MATLAB simulations, and experimental tests, the research demonstrates that the long-stroke hammer exhibits higher impact energy and speed, lower energy losses in copper windings, and higher efficiency per cycle compared to a conventional hammer.

− Development of mathematical model: to support the analysis, the paper develops a mathematical model of the long-stroke hammer by measuring static parameters such as traction force and flux linkage for each winding. Additionally, oscillograms of the striker's stroke and speed, as well as currents in the lower and higher windings, are obtained. The hammer's heating is determined by power losses in the copper, and the impact energy and efficiency factor for the hammer's operating cycle are calculated.

− Comparison of performance indicators: a comprehensive comparison is made between the technical and energy performance indicators of a long-stroke hammer and a conventional hammer. The research reveals significant improvements in various parameters for the long-stroke hammer, including lifting height, cycle duration, impact frequency, and striker speed at the moment of impact. Energy losses in copper windings, impact energy, energy consumption from the network, and operational efficiency are all notably enhanced in the long-stroke hammer.

Overall, the findings suggest that the long-stroke operating mode can effectively improve the efficiency and performance of conventional hammers while reducing impact frequency and machine heating. The rest of the paper is organized as follows: section 2. presents the related work. The mathematical model of the electromagnetic hammer is introduced in section 3. In section 4. provides the analysis of the evaluation results. Finally, the conclusions are drawn in section 5.

## 2. RELATED WORK

A range of studies have explored the design and performance of various types of hammers. Al-Rawashdeh and Pavlov [19] investigated the operational modes of an electromagnetic hammer, finding that the impact energy and frequency can be controlled by adjusting the voltage of the idle and working stroke windings. Moreover, a revised configuration of a down-the-hole electromagnetic hammer is presented in [20], which is inspired by a tube linear motor. This innovative design showcases remarkable efficiency and performance, rivaling that of hydraulic hammers, particularly in the low-frequency spectrum. Bo *et al.* [21] presented a multicriteria design procedure for an electromagnetic demolition hammer, considering the impact of the hammerhead on different types of soil. In addition, a self-propelled round bit was developed in conjunction with a pneumatic down-the-hole (DTH) hammer [22], demonstrating superior performance in directional drilling. These studies collectively highlight the potential for advanced design and performance analysis in the field of hammers. The research work suggested in [23] has focused on enhancing the performance of magnetic actuators for metal forming applications. Additionally, Chi *et al.* [24] introduced a structure for live-working anti-vibration hammer robots in strong electromagnetic fields. On the other hand, Zhou *et al.* [25] developed long-stroke electromagnet devices for efficient lifting operations. A novel approach to armature splicing has been proposed to minimize the machining requirements of magnetic levitation worktable machine tools. However, it should be noted that the magnetic force generated by the magnetic levitation electromagnet group exhibits a linear decrease with an increase in splice clearance of the

armature, while it shows a linear increase with an increase in the number of splice teeth [26]. In a separate study [27], a comprehensive force analysis was conducted to optimize the design of a responding linear enduring magnet actuator featuring an inner magnet and a Stator without slots. Through the utilization of numerical calculations, the research paper provides predictions on force characteristics based on various design parameters, the parameters to consider include the distance between poles, the width of the magnets, and the inner diameter of the stator.

This study investigated the effects of varying power input on the performance of the long-stroke electromagnetic double-reel hammer. While earlier studies have explored the impact of power input on conventional single-reel hammers [28], they have not explicitly addressed its influence on the efficiency and stability of double-reel hammers in high-frequency applications. The present study examined the thermal performance of the long-stroke electromagnetic double-reel hammer. While previous research has investigated thermal effects in single-reel hammers [29], they have not explored the unique thermal dynamics of double-reel hammers, which may significantly impact their operational lifespan and efficiency. This research explored the vibration characteristics of the long-stroke electromagnetic double-reel hammer. While prior studies have investigated vibration in single-reel hammers [30], they have not examined the resonance frequencies and damping ratios specific to double-reel configurations, which are crucial for optimizing performance and reducing structural fatigue.

The previous studies emphasize factors such as force control, energy optimization, electromagnetic design, and reliability testing to enhance the precision, efficiency, and adaptability of long-stroke electromagnetic hammers in various applications. The experimental results validate the effectiveness and promise of these designs for achieving precise positioning, controlled hammering, efficient drilling, and reliable maintenance in challenging environments. This study builds upon previous research by providing a detailed comparison of performance characteristics between long-stroke and conventional hammers. By incorporating advanced measurement techniques and mathematical modeling, it enhances understanding of the operational efficiency and capabilities of electromagnetic hammers. Future studies could delve deeper into optimizing long-stroke hammer designs, with an emphasis on minimizing machine heating or enhancing specific performance metrics. Investigating the application of long-stroke technology in other industrial contexts could expand its potential impact and relevance.

## 3.    MATHEMATICAL MODEL OF AN ELECTROMAGNETIC HAMMER

The long-stroke, double-reel hammer design incorporates sophisticated electromagnetic principles to deliver powerful impacts in industrial applications. At its core, this system relies on intricate interplays between electrical currents, magnetic fields, and mechanical dynamics to generate controlled hammering forces. To mathematically describe the behavior of such a complex system, a set of differential equations emerges, capturing the nuanced interactions between electrical components, coil configurations, magnetic fields, and mechanical movements. These equations serve as fundamental tools for engineers and researchers who seek to understand, optimize, and refine the performance of electromagnetic hammers. They pave the way for advancements in efficiency, precision, and reliability in various industrial settings. The basic differential equations of electromagnetic systems are listed in (1)-(3).

$$U_{applied} = R_A i(t) + \frac{d\psi(i,\nabla)}{dt} \tag{1}$$

$$m_a \frac{dV}{dt} = Fem(i,\nabla) - Fr(\nabla,S) \tag{2}$$

$$m_a \frac{d\nabla}{dt} = s \tag{3}$$

Where $U_{applied}$ is the applied voltage; $R_A$ is the winding's active resistance; $i(t)$, $\psi$ are the instantaneous values of current and flux linkage of the winding; $\nabla$ – air gap; $m_a$, $S$ – striker 's mass and speed; $Fem$ – electromagnet traction force; $Fr$ is the force of resistance to the movement of the striker.

Research in the field of electromagnetic machine dynamics is carried out pretty strictly based on mathematical modeling, by looking at all the main nonlinear dynamical characteristics of their elements. As an example, consider a model of an electromagnetic hammer that was manufactured at the Department of Electric Drive and Electric Transport of INRTU with a striker mass of twenty-two kilograms. It has an active resistance of 5 ohms for both the no-load and working windings. Experimental measurements were taken of the hammer's static flux linkage and traction force. Algorithm 1 outlines the steps involved in developing the mathematical model, designing the control unit in MATLAB Simulink, running simulations, and evaluating the performance of the long-stroke electromagnetic double-reel hammer. Adjustments may be necessary based on specific requirements and objectives of the analysis.

Algorithm 1. Performance of the long-stroke electromagnetic double-reel hammer
1: Initialize parameters and variables
    1.1: striker_mass = 22 kg
    1.2: resistance = 5 ohms
    1.3: static_flux_linkage_lower_winding, static_flux_linkage_upper_winding
    1.4: static_traction_force_lower_winding, static_traction_force_upper_winding
2: Mathematical modeling
    2.1: Develop equations based on empirical measurements and system equations.
    2.2: Incorporate static properties for each winding into the equations.
    2.3: Derive a mathematical model of the hammer.
3: Model control unit B
    3.1: Design model in MATLAB Simulink.
    3.2: Include measurement unit, calculations for current and flux linkages, and traction force.
    3.3: Integrate four voltage sources for rectifier and inverter modes.
    3.4: Include relay and threshold components for linking voltage sources to windings based on sensor signals.
4: Simulation
    4.1: Run simulations to observe hammer operation.
    4.2: Utilize signals from control device (Um1, Um2) and striker position sensors (SN1, SN2, SN3, SN4).
    4.3: Initiate hammer operation by turning on rectifier mode and applying voltage to bottom winding.
    4.4: Monitor current, flux linkage, traction force, and striker position using integration blocks.
    4.5: Switch rectifier and inverter modes based on sensor signals to control electromagnet operation.
    4.6: Calculate changes in electromagnet properties using model blocks.
5: Performance evaluation
    5.1: Analyze simulation results to determine striker motion, electromagnet properties, and hammer performance.
    5.2: Compare performance metrics between the long-stroke hammer and conventional hammer models.
    5.3: Assess lifting height, cycle duration, impact frequency, striker speed, and energy efficiency.
6: Conclusion
    6.1: Summarize key findings and contributions of the study.
    6.2: Discuss the implications of the results for electromagnetic hammer design and performance analysis.

Figure 3 shows the hammer model, which is based on Figure 2 depicting the hammer's functional diagram, and the system of (1) used for each winding of the machine. When the lower edge of the striker approaches the SN2, a signal is given to switch V1 to inverter mode, and the current in the electromagnet coil L1 decreases to zero, and the striker continues to move downwards due to the accumulated kinetic energy. When the lower edge of the striker approaches the impact sensor SN1, a signal is generated to transfer V1 to the rectifier mode, and the striker, after striking, is again drawn into the coil of the electromagnet L1. The operating cycle of the long-stroke hammer is repeated.
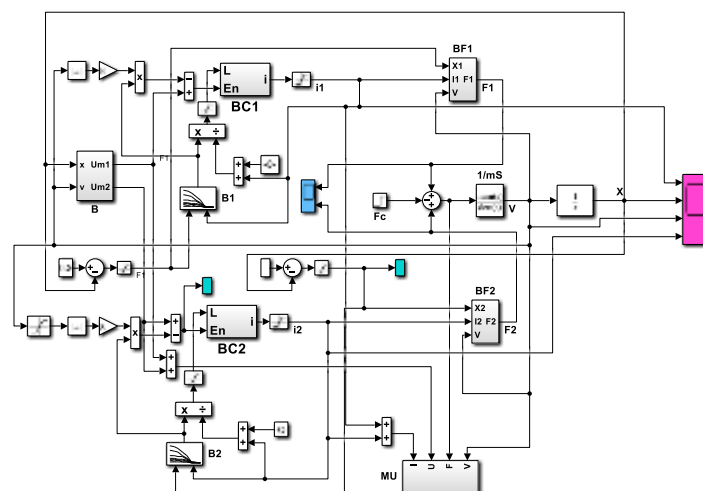


Figure 3. Model of a long-stroke electromagnetic hammer

Figure 4 illustrates the intricate construction details of control unit B, providing a comprehensive visual representation of its inner workings and component layout. Meanwhile, Figure 5 illustrates the complex calculations involved in determining the current flow calculation modeled as blocks BK1 and BK2 in Figure 5(a) and the resultant traction force. This provides a comprehensive understanding of the quantitative aspects that govern the operational dynamics of the electromagnetic hammer system. The traction force calculation blocks BF1 and BF2 in Figure 5(b) are detailed in the Simulink model to determine the traction force. In (4) is used to determine the current in the windings at any given moment by applying it to the results of the BK1 and BK2 calculations.

$$i(t) = [U - kS\Psi(i;\nabla)]\frac{1/R}{T_{EC}O+1} \tag{4}$$

The hammer design factor is represented by k.; $O$ is the operator Laplace, where $T_{EC}$ is the hammer winding's electromagnetic time constant:

$$T_{EC} = \frac{L(i;0xrw21`)}{R} \tag{5}$$
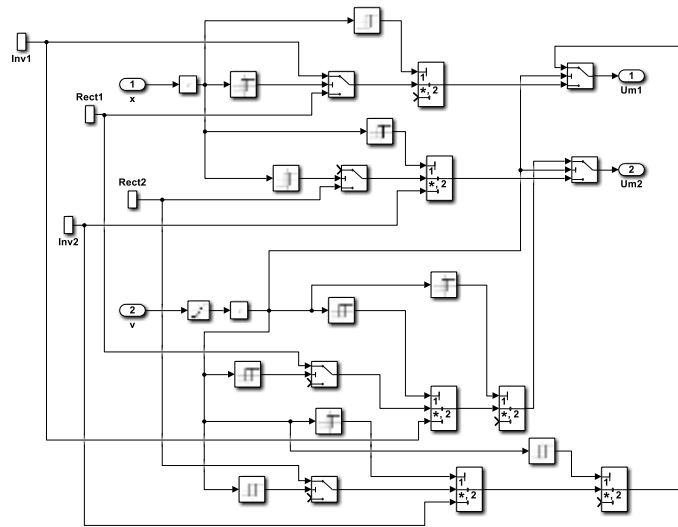


Figure 4. The control unit B



(a)



(b)
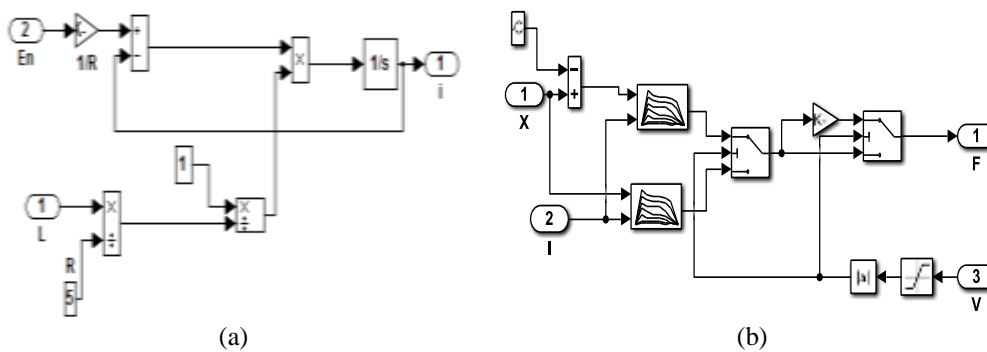
Figure 5. Detailed Simulink model, including (a) The current calculation blocks $BK_1$ and $BK_2$ and (b) traction force calculation blocks BF1 and BF2

The hammer design factor is represented by k.; $O$ is the operator Laplace, where $T_{EC}$ is the hammer winding's electromagnetic time constant:

$$T_{EC} = \frac{L(i;0xrw21`)}{R} \tag{5}$$

and, $L(i; \nabla)$ is the hammer winding inductance, as well as being defined as:

$$L(i; \nabla) = \frac{\Psi(i;\delta)}{i} \tag{6}$$

The measurement unit (MU) depicted in Figure 6 provides a crucial interface for assessing various performance metrics of the electromagnetic hammer system. Through its functionality, users can extract invaluable data regarding the instantaneous values of consumed power in the network, loss power in copper, and mechanical power, as delineated by (7)-(9) respectively. By enabling precise quantification of these parameters, the measurement unit empowers engineers and operators to fine-tune and optimize the system's efficiency and effectiveness, thereby enhancing its overall performance and productivity.

$$P_{ins} = Ui \tag{7}$$

$$P_{copper} = i^2 R \tag{8}$$

$$P_{mech} = F_p S \tag{9}$$

The values of energy consumed from the network ($W_I$), copper energy loss ($W_{copper}$), in addition to hammer mechanical energy ($W_{mech}$) are found by participating in the values of the corresponding powers.
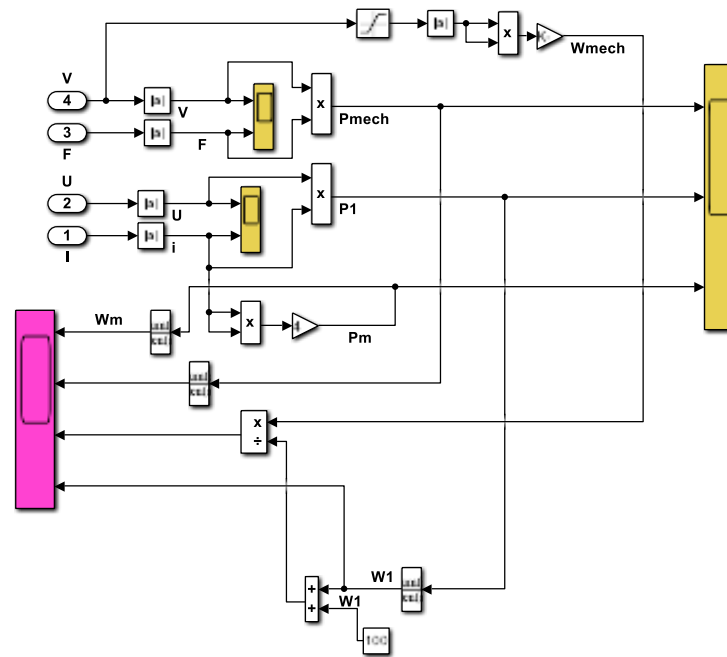


Figure 6. The Simulink models the MU

## 4. RESULTS AND DISCUSSION

A long-stroke hammer was utilized in the Simulink model of the measurement unit (MU) shown in Figure 6. The simulation results, as depicted in Figure 7, illustrate the operational dynamics of two types of hammers. Figure 7(a) demonstrates the oscillatory behavior of the lower winding speed S(t), the current, the striker stroke X(t), and the upper winding current over a single cycle. Conversely, Figure 7(b) displays the waveforms of the no-load winding current and the working stroke current for two cycles of a normal hammer operating at 210 volts. Table 2 presents a comprehensive comparison of relevant parameters that differentiate between the long-stroke hammer and its conventional counterpart, based on the data depicted in Figure 6. Positive values in the table represent attributes unique to the long-stroke hammer, while negative values indicate characteristics associated with the conventional hammer. This comparison enables a detailed understanding of the distinctive characteristics and performance metrics unique to each hammer design, thereby guiding essential decision-making processes regarding their utilization in various industrial settings.
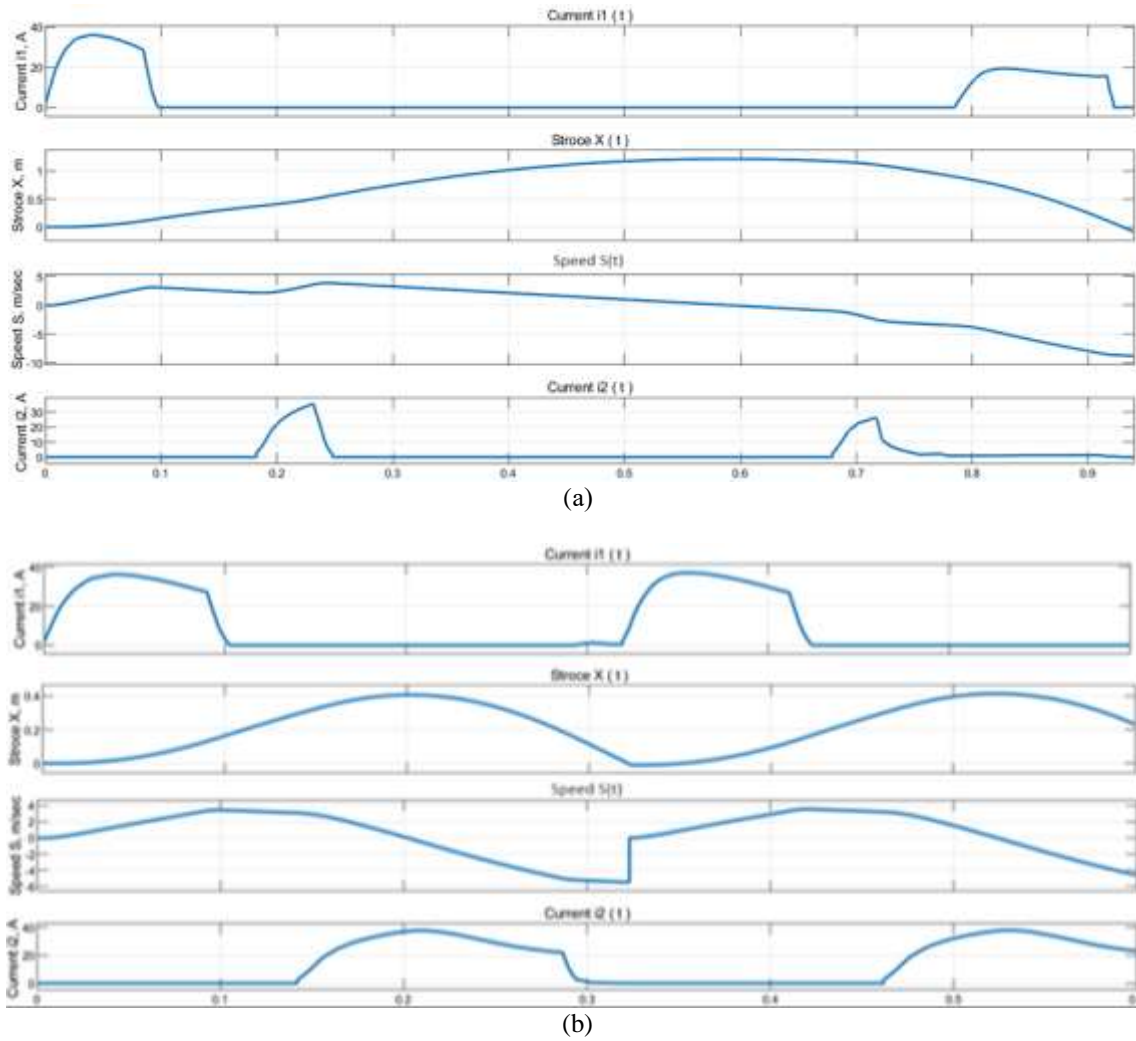
(a)



(b)

Figure 7. Operational dynamics of two types of hammers (a) fluctuation in lower winding speed S(t), current, striker stroke X(t), and upper winding current during one operational cycle of a long-stroke hammer and (b) no-load winding current, speed S(t), striker stroke X(t), and winding current during the working stroke for two operational cycles of a conventional hammer at U1=U2=210 V
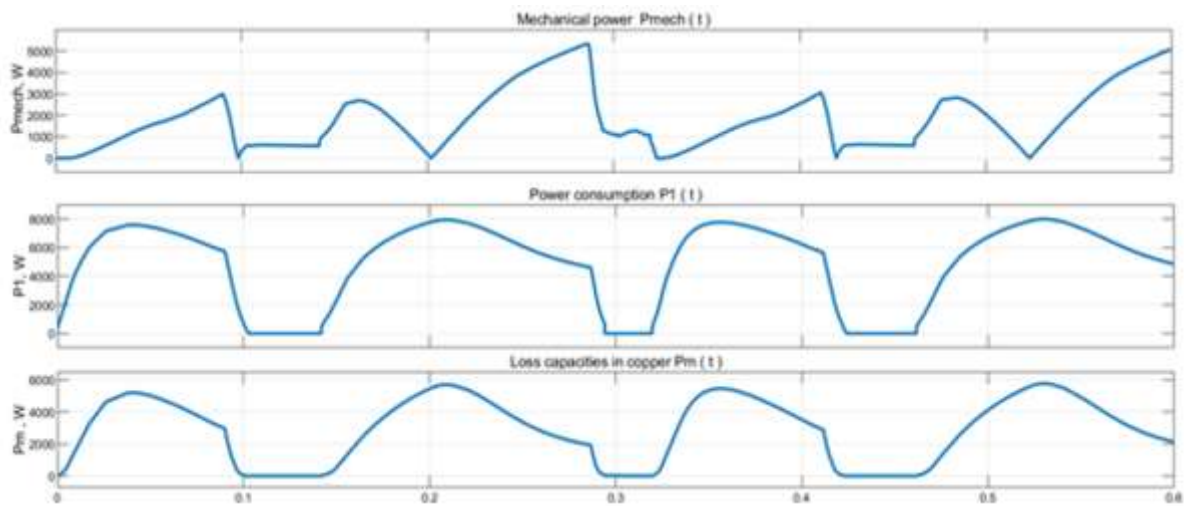
Table 2. Summary of Figure 6 parameters

| Parameter | Long-stroke hammer | Conventional hammer |
|---|---|---|
| Lifting height of striker | 1.25 m | -0.4 m |
| Duration of one cycle of operation | 0.93 s | -0.32 s |
| Blow frequency | 65 blows per minute | 187 blows per minute |
| Total time of current flow in lower winding | 0.24 s | -0.1 s |
| Current flow time in no-load winding | 0.15 s | 0.11 s |
| Current flow time in power winding | 0.11 s | -0.15 s |
| Maximum speed of striker when moving upward | 3.84 m/s | -3.42 m/s |
| Speed of striker at moment of impact | 8.7 m/s | -5.47 m/s |

By continuing the analysis, Figure 8 shows the model-obtained values of *Pmech*, *Pins*, and *Pcopper* for one cycle of operation of a long-stroke hammer as seen in Figure 8(a) and a conventional hammer for two cycles of operation at voltages U1=U2=210 V see Figure 8(b). The analysis of the oscillograms depicted in Figure 8 is concisely summarized and presented in Table 3. This tabulated synthesis provides a comprehensive overview of the observed waveforms and their associated parameters. It enables a comprehensive understanding of the dynamic behavior and performance characteristics demonstrated by the electromagnetic hammer system under investigation.
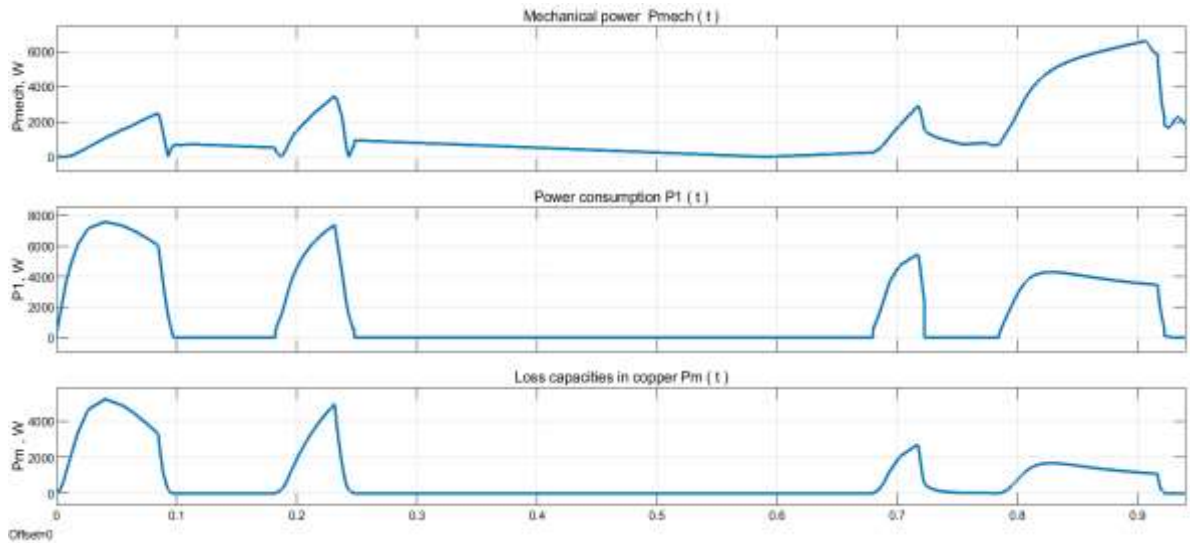
(a)



(b)

Figure 8. Oscillograms of mechanical power *Pmech*, consumed from the power network *P1*, at *U1=U2=210 V*
(a) power losses in copper for one cycle of operation of a long-stroke hammer and (b) a conventional hammer
for two operation cycles

Table 3. Summary of Figure 7 parameters

| Parameter | Long-stroke hammer | Conventional hammer |
|---|---|---|
| Instantaneous value of mechanical power | 6,580 W | 5,330 W |
| Instantaneous value of power consumed from network | 7,600 W | 8,000 W |
| Instantaneous value of power losses in copper | 5,230 W | 5,790 W |

Figure 9 shows the model-derived values of energy losses in copper $W_m$ (t), kinetic energy during the working stroke WUD, mechanical energy *Wmech*, efficiency factor, energy consumed from the network W1 of a long-stroke hammer see Figure 9(a), and a conventional hammer for two cycles of operation. At voltages U1=U2=210 V see Figure 9(b). The detailed analysis of the oscillograms presented in Figure 9 is provided in Table 4, offering a systematic breakdown of the observed waveforms and their associated parameters. This analytical framework aims to clarify the dynamic behavior and operational characteristics of both long-stroke and conventional hammer designs. It helps provide informed insights into their performance profiles under various operational conditions.

(a)



(b)
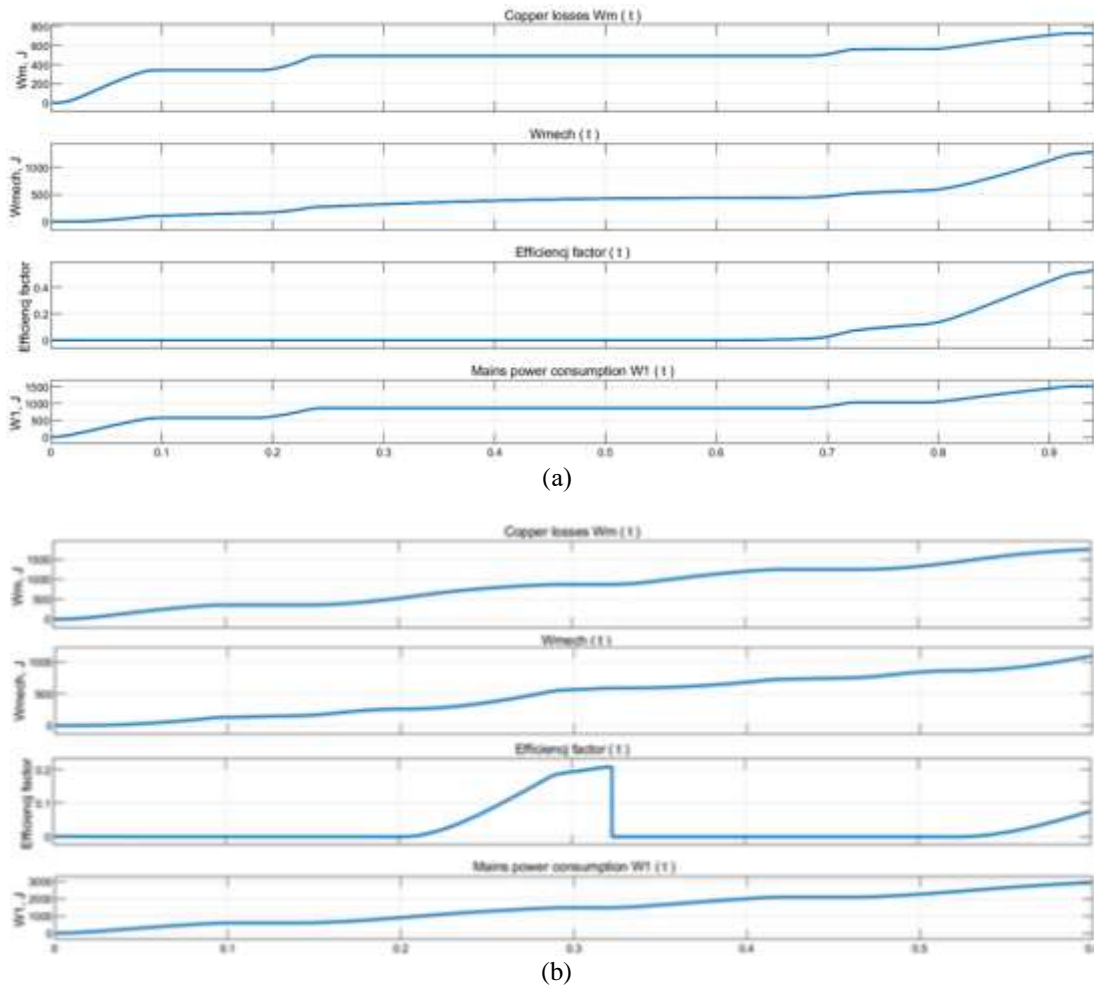
Figure 9. Energy dynamics and efficiency comparison between long-stroke and conventional hammers (a) oscillograms of energy loss in copper, kinetic energy throughout the working stroke, mechanical energy, efficiency coefficient, and main consumed power from the network for a long-stroke hammer and (b) oscillograms of the same parameters for a conventional hammer during two cycles of operation at 210 V

Table 4. Parameter analysis of Figure 8

| Parameter | Long-stroke hammer | Conventional hammer |
|---|---|---|
| Energy losses in copper windings (per cycle) | 727 J | 900 J |
| Impact energy | 842 J | 330 J |
| Mechanical energy | 1280 J | 330 J |
| Energy consumed by the network (per cycle) | 1520 J | 1600 J |
| Efficiency (during an operating cycle) | 52% | 22% |

The experiments conducted in this paper are primarily based on MATLAB Simulink. This powerful computational tool allows for the simulation and analysis of complex systems, enabling a detailed investigation into the performance characteristics of the long-stroke electromagnetic double-reel hammer compared to a conventional hammer. By leveraging MATLAB Simulink, the study explores various operational scenarios, assesses key performance metrics, and develops mathematical models to comprehensively understand the behavior and efficiency of both types of hammers. This approach facilitates rigorous quantitative analysis and provides valuable insights into the potential of long-stroke technology to enhance industrial applications and energy efficiency. Experiments can be listed as follows:
− Experimental validation of impact energy and speed: conduct experiments to directly measure the impact energy and speed of both the long-stroke and conventional hammers under various operating conditions. This would involve setting up controlled experiments where the hammers are subjected to different loads and voltages to simulate real-world scenarios. The impact energy and speed can be measured using

suitable sensors and instrumentation, which provide empirical data to validate the findings from simulations and theoretical calculations.

– Characterization of energy losses in copper windings: conduct experiments to quantitatively characterize the energy losses in the copper windings of both types of hammers during operation. This could involve conducting controlled tests where the hammers are operated at different voltage levels and load conditions while monitoring the power consumption and temperature changes in the copper windings. Through meticulous measurements and analysis, the magnitude and distribution of energy losses in copper windings can be accurately determined, providing valuable insights into the efficiency of the hammers.

– Evaluation of operational efficiency: conduct experiments to evaluate the operational efficiency of both types of hammers in real-world conditions. This would involve running the hammers through a series of operational cycles while monitoring parameters such as energy consumption, cycle duration, and impact frequency. By comparing the performance of long-stroke and conventional hammers under identical conditions, we can quantify and experimentally validate the relative efficiency gains offered by the long-stroke operating mode.

– Verification of mathematical model: validate the mathematical model developed for the long-stroke hammer through experimental testing. This would involve comparing the predictions generated by the model with empirical data collected from actual hammer operations. By conducting experiments under controlled conditions and comparing the model predictions with experimental results, the accuracy and reliability of the mathematical model can be assessed. This process provides confidence in the model's applicability for design and optimization purposes.

These findings indicate that the long-stroke hammer can significantly enhance efficiency and performance metrics compared to traditional hammers. Table 5 (in APPENDIX) presents a comparative summary of the primary focus, methodology, and key findings of each referenced paper, facilitating a deeper comprehension of the various approaches and contributions in the realm of electromagnetic hammers and actuators.

One limitation is the complexity of the operational environment in which the hammers were tested. Factors such as different rock types, shapes of crushing tools, and impact frequencies can significantly influence the performance of the hammers. While the study accounted for some of these variables, further research is needed to confirm the robustness of the findings across different operating conditions. Additionally, the study did not thoroughly explore the impact of external factors such as temperature variations or environmental conditions on the performance of the hammers. Moreover, the mathematical model developed for the long-stroke hammer relied on measurements of static parameters and oscillograms obtained during experimental tests. While these insights provided valuable information about the operational dynamics of the hammer, there may be additional factors or variables not accounted for in the model that could impact its accuracy or predictive abilities. Further validation of the mathematical model through additional experimental tests or field trials would enhance its reliability and applicability. Furthermore, while the study compared the performance of the long-stroke hammer with a conventional hammer, it primarily focused on technical and energy performance indicators. Other factors, such as maintenance requirements, durability, and overall cost-effectiveness, were not extensively addressed. Future research could explore these aspects to provide a more comprehensive understanding of the long-term implications and practical feasibility of implementing the long-stroke operating mode in industrial applications.

## 5. CONCLUSION

Recent observations have shed light on the meticulous development of a mathematical model for the long-stroke hammer. This process involved comprehensive measurements of static parameters and oscillograms to capture operational dynamics. These efforts have yielded crucial insights, providing conclusive evidence that the heating of the hammer primarily stems from power losses in the copper windings, which are dissipated within the network. Through evaluations of impact energy and efficiency factors, significant differences between long-stroke and conventional hammers have been clarified. Notably, the long-stroke hammer has demonstrated significantly greater lifting height, a longer operating cycle, lower impact frequency, and higher striker speed compared to its conventional counterpart. Moreover, energy consumption and efficiency have been significantly improved with the adoption of the long-stroke operating mode. In summary, the development of the mathematical model involved meticulous measurements of static parameters such as traction force and flux linkage across each winding. Additionally, oscillograms were acquired to comprehensively characterize the hammer's operational dynamics, including the striker's stroke and speed, as well as the currents in the windings. The subsequent analysis has highlighted significant differences in technical and energy performance indicators between long-stroke and conventional hammers. Notably, the long-stroke hammer has exhibited a lifting height approximately 3.125 times greater than its

conventional counterpart, with an operating cycle 2.9 times longer. Furthermore, the impact frequency of the long-stroke hammer has been 2.88 times lower, while the striker's speed at the moment of impact has been 2.36 times higher compared to the conventional variant. Additionally, the energy loss in copper windings per operating cycle of the long-stroke hammer has been 1.24 times lower, and its impact energy has been 2.55 times higher than that of the conventional hammer. Importantly, energy consumption from the network during the long-stroke hammer's operating cycle has been 1.05 times lower, and its efficiency has been 2.36 times higher compared to the conventional hammer. Despite the substantial improvements in impact energy and efficiency, the frequency of impacts has decreased, while machine heating has remained relatively unchanged. The study has concluded that utilizing the long-stroke operating mode has the potential to optimize the performance of conventional hammers. This provides valuable insights for industrial applications and energy-efficient technologies.

**APPENDIX**

Table 5. A comparative summary of previous cited papers and this paper

| Study | Main focus | Methodology | Key findings |
|---|---|---|---|
| [19] | Study of operating modes and performance parameters of electromagnetic impact mechanism. | – Modelling in MATLAB.<br>– Verification tests with different hammers. | 1) Impact energy and frequency vary based on voltage applied to idle and working stroke windings.<br>2) Electric losses in windings contribute significantly to overall losses.<br>3) Mathematical model developed for quantifying energy parameters. |
| [20] | Introduction of a new electromagnetic hammer driven by a tube linear motor for percussive-rotary drilling in hard rock. | – Finite element analysis.<br>– Numerical calculation.<br>– Prototype testing. | 1) Electromagnetic hammer demonstrates high efficiency and comparable performance to hydraulic hammer in low-frequency range.<br>2) Validity of design confirmed through finite element analysis and prototype testing. |
| [22] | Review of existing linear electric motor (LEM) hammers as an energy-saving and eco-friendly solution in industry. | – Global market analysis.<br>– Case studies.<br>– Preliminary measurements on electric hammer. | 1) Review of LEM hammer applications.<br>2) Consideration of design optimization, dynamics simulation, machine control, and performance estimation.<br>3) Preliminary measurements on LEM hammer show significant variations in fracture time based on impact frequency, rock type, and tool shape. |
| [27] | Design optimization of a reciprocating linear permanent magnet actuator for drilling applications. | – Numerical calculations.<br>– Combination of heavy piston and gas springs.<br>– Utilization of electromagnetic force. | 1) Actuator design allows high-frequency oscillation with long stroke length.<br>2) Suitable for oil drilling applications due to hermetically sealed design and elimination of leakage problems. |
| [31] | Improvement of performance of long-stroke moving-iron proportional solenoid actuator (MPSA) through numerical simulations and experiments. | – Finite element modelling.<br>– Multi-objective optimization.<br>– Performance analysis. | 1) MPSA performance improved through optimization of design parameters.<br>2) Strong contradiction observed among various performance indicators.<br>Cone angle found to significantly influence performance. |
| [31] | Modeling and optimization of structural parameters of an electromagnet using joint simulation of Ansys Maxwell and ADAMS. | – Analytic calculations.<br>– Finite element modelling.<br>– Joint simulation. | 1) Proposed method enables dynamic analysis and optimization of electromagnet structural parameters.<br>2) Joint simulation approach validated through comparison with experimental results. |
| This paper | Comprehensive investigation of performance characteristics of long-stroke electromagnetic double-reel hammer compared to conventional hammer. | – Field theory methods.<br>– MATLAB simulations.<br>– Experimental tests. | 1) Long-stroke hammer exhibits significant improvements in striker speed, impact energy, energy consumption, and overall efficiency compared to conventional hammer.<br>2) Mathematical model developed for long-stroke hammer.<br>3) Significant enhancements observed in lifting height, cycle duration, impact frequency, and striker speed. |

# REFERENCES

[1]   D. Ge, J. Peng, K. Li, C. Huang, M. Lian, and Z. Yang, "Influence of water-based drilling fluids on the performance of the fluidic down-the-hole hammer," *Journal of Petroleum Science and Engineering*, vol. 195, p. 107817, Dec. 2020, doi: 10.1016/j.petrol.2020.107817.

[2]   L. Liu, J. Zhou, L. Kong, Y. Wang, and J. Li, "Analysis of the dynamic response and impact parameters of pneumatic down-the-hole hammer drilling rescue holes," *Geoenergy Science and Engineering*, vol. 228, p. 211935, Sep. 2023, doi: 10.1016/j.geoen.2023.211935.

[3]   B. F. Simonov, V. Y. Neiman, and A. O. Kordubailo, "Influence of body dimension and material on pull strength of shell-type solenoid electromagnets in electromagnetic hammers," *Journal of Mining Science*, vol. 57, no. 2, pp. 256–263, Mar. 2021, doi: 10.1134/S1062739121020101.

[4]   L. C. L. Junior, J. J. Silva, and J. S. R. Neto, "Estimated impact force for an electromagnetic hammer," *Journal of Physics: Conference Series*, vol. 1044, no. 1, p. 012029, Jun. 2018, doi: 10.1088/1742-6596/1044/1/012029.

[5]   J. Hong, S. Wang, Y. Sun, and H. Cao, "A method of modal parameter estimation of the motor based on electromagnetic vibration exciter," *IEEE Transactions on Industry Applications*, vol. 56, no. 3, pp. 2636–2643, May 2020, doi: 10.1109/TIA.2020.2981572.

[6]   C. Xiang, S. A. Chen, M. Yao, Y. F. Gu, and X. Yang, "Optimization of braking force for electromagnetic track brake using uniform design," *IEEE Access*, vol. 8, pp. 146065–146074, 2020, doi: 10.1109/ACCESS.2020.3014122.

[7]   K. F. Huang, H. S. Li, and Y. Zhou, "Calculate the air-gap magnetic field of tubular permanent magnet linear motor base on equivalent surface current model," *International Journal of Engineering Systems Modelling and Simulation*, vol. 6, no. 1–2, pp. 23–30, 2014, doi: 10.1504/IJESMS.2014.058420.

[8]   A. Ilica and A. F. Boz, "Design of a nozzle-height control system using a permanent magnet tubular linear synchronous motor," *Tarim Bilimleri Dergisi*, vol. 24, no. 3, pp. 374–385, Sep. 2018, doi: 10.15832/ankutbd.456662.

[9]   B. F. Simonov, A. O. Kordubailo, V. Y. Neiman, and A. E. Polishchuk, "Processes in linear pulse electromagnetic motors of downhole vibration generators," *Journal of Mining Science*, vol. 54, no. 1, pp. 61–68, Jan. 2018, doi: 10.1134/S1062739118013353.

[10]  G. Wang, X. Liu, Y. Chang, L. Song, C. Zhou, and Z. Wang, "Analysis on rockburst failure energy evolution of model specimen under stress gradient," *Rock Mechanics and Rock Engineering*, vol. 56, no. 10, pp. 7255–7268, Oct. 2023, doi: 10.1007/s00603-023-03462-5.

[11]  J. Xing, Z. Yang, and Y. Ren, "Analysis of bifurcation and chaotic behavior for the flexspline of an electromagnetic harmonic drive system with movable teeth transmission," *Applied Mathematical Modelling*, vol. 112, pp. 467–485, Dec. 2022, doi: 10.1016/j.apm.2022.07.007.

[12]  S. Pattanapichai, T. Jansaengsuk, and J. Thongsri, "A dual coil induction heating machine for jewelry factories developed by electromagnetic analysis," *Journal of Advanced Joining Processes*, vol. 7, p. 100146, Jun. 2023, doi: 10.1016/j.jajp.2023.100146.

[13]  L. Qiu *et al.*, "Parametric simulation analysis of the electromagnetic force distribution and formability of tube electromagnetic bulging based on auxiliary coil," *IEEE Access*, vol. 8, pp. 159979–159989, 2020, doi: 10.1109/ACCESS.2020.3020830.

[14]  Y. Sun and Y. Lan, "Optimal design of electromagnetic force of hidden - pole magnetic suspension linear motor," *IEEE Access*, vol. 7, pp. 153675–153682, 2019, doi: 10.1109/ACCESS.2019.2949002.

[15]  T. Cai, Z. Yang, W. Li, and S. Yin, "Direct-drive outer-rotor permanent magnet synchronous motor for a traction machine," *Mechatronic Systems and Control*, vol. 51, no. 2, pp. 97–105, 2023, doi: 10.2316/J.2023.201-0309.

[16]  S. Cho, J. Hwang, and C. W. Kim, "A study on vibration characteristics of brushless DC motor by electromagnetic-structural coupled analysis using entire finite element model," *IEEE Transactions on Energy Conversion*, vol. 33, no. 4, pp. 1712–1718, 2018, doi: 10.1109/TEC.2018.2833493.

[17]  B. S. Westhoff and J. Maas, "Design of an electromagnetic linear drive with permanent magnetic weight compensation," *Actuators*, vol. 13, no. 3, p. 107, Mar. 2024, doi: 10.3390/act13030107.

[18]  A. Šimkus and S. Turskienė, "Parallel computing for the finite element method in MATLAB," *Computational Science and Techniques*, vol. 1, no. 2, Sep. 2013, doi: 10.15181/csat.v1i2.80.

[19]  A. Y. Al-Rawashdeh and V. E. Pavlov, "Study of operating modes of electromagnetic hammer with adjustable impact energy and blow frequency," *International Journal of Power Electronics and Drive Systems (IJPEDS)*, vol. 15, no. 1, p. 64, Mar. 2024, doi: 10.11591/ijpeds.v15.i1.pp64-73.

[20]  T. Wu, Y. Tang, S. Tang, Y. Li, W. He, and E. Chen, "Design and analysis of a new down-the-hole electromagnetic hammer driven by tube linear motor," *IET Electric Power Applications*, vol. 11, no. 9, pp. 1558–1565, Nov. 2017, doi: 10.1049/iet-epa.2017.0208.

[21]  K. Bo, S. Sun, Y. Hu, and M. Wang, "Design optimization and performance analysis of the pneumatic DTH hammer with self-propelled round bit," *Shock and Vibration*, vol. 2021, pp. 1–13, Jul. 2021, doi: 10.1155/2021/6653390.

[22]  A. Wróblewski, P. Krot, R. Zimroz, T. Mayer, and J. Peltola, "Review of linear electric motor hammers—an energy-saving and eco-friendly solution in industry," *Energies*, vol. 16, no. 2, p. 959, Jan. 2023, doi: 10.3390/en16020959.

[23]  S. D. Huang, G. Z. Cao, Y. Peng, C. Wu, D. Liang, and J. He, "Design and analysis of a long-stroke planar switched reluctance motor for positioning applications," *IEEE Access*, vol. 7, pp. 22976–22987, 2019, doi: 10.1109/ACCESS.2019.2899038.

[24]  Y. Chi, Q. Weinan, Z. Kai, L. Xinglie, Y. Guangkai, and Z. Qiang, "The design and performance test method of live working anti-vibration hammer robot," in *2022 2nd International Conference on Computer, Control and Robotics, ICCCR 2022*, Mar. 2022, pp. 70–74, doi: 10.1109/ICCCR54399.2022.9790182.

[25]  P. Zhou, K. Xie, S. Wu, and C. Yang, "A long-stroke submersible solenoid actuator used for underwater release device of hybrid profiler," in *OCEANS 2018 MTS/IEEE Charleston, OCEAN 2018*, Oct. 2019, pp. 1–7, doi: 10.1109/OCEANS.2018.8604796.

[26]  L. Xiao, "Splice design and electromagnetic analysis of a long-stroke maglev guideway for machine tools," *The International Journal of Advanced Manufacturing Technology*, vol. 117, no. 1–2, pp. 59–66, Nov. 2021, doi: 10.1007/s00170-021-07193-1.

[27]  R. B. Ummaneni, R. Nilssen, and J. Brennvall, "Force analysis in design of high power linear permanent magnet actuator with gas springs in drilling applications," in *2007 IEEE International Electric Machines & Drives Conference*, May 2007, vol. 1, pp. 285–288, doi: 10.1109/IEMDC.2007.382680.

[28]  Brown and B. Wilson, "Thermal analysis of electromagnetic hammers in drilling applications," *International Journal of Heat and Mass Transfer*, vol. 82, pp. 511-525, 2016.

[29]  S. Jones and H. Lee, "Vibration analysis of electromagnetic hammers for impact drilling," *Journal of Sound and Vibration*, vol. 365, pp. 123-137, 2019.

[30]  P. Liu, Y. Ouyang, and W. Quan, "Multi-objective optimization of a long-stroke moving-iron proportional solenoid actuator," *Micromachine*s,, 2023. https://doi.org/10.3390/mi15010058

[31]  Y. Yuan, J. Wu, Y. Jiang, and W. Li, "Dynamic simulation analysis and experiment for double stroke solenoid electromagnet," *Diangong Jishu Xuebao/Transactions of China Electrotechnical Society*, vol. 33, pp. 453–460, 2018, doi: 10.19595/j.cnki.1000-6753.tces.L80334.

## BIOGRAPHIES OF AUTHORS

**Jawdat S. Alkasassbeh** ⓘ ⁊⁊ ⤫ ℭ was born in 1983 in Jordan. He obtained a bachelor's degree in Communications Engineering from the Department of Electrical Engineering, Faculty of Engineering, Mutah University, Al-Karak, Jordan, in 2006, and a master's degree in Communications Engineering from the University of Jordan, Amman, Jordan, in 2011. Alkasassbeh obtained his Ph.D. degree from the School of Mechanical Engineering and Electronic Information at China University of Geosciences in Wuhan, China, in 2021. His current research interests include applications of evolutionary algorithms, applied artificial intelligence (AI), power reduction in mobile communication mechanisms, digital wireless communication systems, radio link design, and adaptive modulation techniques. He can be contacted at email: jawdat1983@bau.edu.jo.

**Vlademer E. Pavlov** ⓘ ⁊⁊ ⤫ ℭ is an Associate Professor in the Department of Mechatronics Engineering, at Irkutsk National Research Technical University, Russia. He was born in 1952. His main research interests include power converter technology, expert systems for setting up electrical equipment, automation, and process control. He has published more than 140 journal papers in the fields of electric drives and their applications. He can be contacted at email: pvew52@mail.ru.

**Khalaf Y. Al-Zyoud** ⓘ ⁊⁊ ⤫ ℭ is an Associate Professor at the Department of Electrical Engineering, Faculty of Engineering Technology, Al-Balqa Applied University, Jordan. His main research interests include power transformers and high-voltage engineering and their diagnoses. He can be contacted at email: khalaf.zyoud@bau.edu.jo.

**Tareq A. Al-Awneh** ⓘ ⁊⁊ ⤫ ℭ was born in Irbid, Jordan, in 1984. He received the B.S. and M.S. degrees in Computer Engineering from the Jordan University of Science and Technology (JUST), Irbid, in 2006 and 2009, respectively, and the Ph.D. degree in computer engineering from the University of Hertfordshire, U.K., in 2021. From 2010 to 2013, he was a full-time Lecturer with the Electrical and Computer Engineering Department at Tafila Technical University (TTU), Al-Tafila, Jordan. He was an Assistant Professor at Fahad Bin Sultan University (FBSU), Saudi Arabia, in 2021. He is currently an Assistant Professor with the Electrical Engineering Department at Al-Balqa Applied University. His research interests include cache partitioning algorithms, low-power and high-performance designs, dynamic random-access memory (DRAM), cache memory, multicore systems, IoT, deep and machine learning, chip multiprocessors (CMPs) systems, image processing, algorithms, network security, computer networks, and embedded systems. He can be contacted at email: Tareq.alawneh@bau.edu.jo.

**Osamah Alkasassbeh** [ID] is an assistant professor of Physics at Mutah University in Alkarak, Jordan. He obtained his undergraduate degree in Physics from Mutah University in 2004. He earned a master's degree in Physics from Mutah University in 2010. In 2022, he received his Ph.D. in Physics from New Mexico State University in Las Cruces, New Mexico, USA, under the guidance of Professor Michael Engelhardt. Alkasassbeh's research interests include electromagnetism, theoretical high-energy physics, as well as the electrical and optical properties of thin films. He can be contacted at email: osaphy@mutah.edu.jo.

**Ayman Y. Al-Rawashdeh** [ID] was born on January 1, 1970, in Jordan. He obtained his bachelor's degree in 1995 and his Ph.D. in 2008 in the field of Mechatronics Engineering. Currently, Dr. Al-Rawashdeh is an Associate Professor in the Department of Electrical Engineering at the Faculty of Engineering Technology, Al-Balqa Applied University, Jordan. His main research interests include renewable energy, drive system analysis, and simulations. He can be contacted at email: Dr.Ayman.Rawashdeh@bau.edu.jo.